[24]D. Van Vliet, AERE Report No. R6395 (unpublished).
[25]T. S. Noggle and J. H. Barrett, Ref. 5, p. 402.
[26]L. C. Feldman, B. R. Appleton, and W. L. Brown, Ref. 5, p. 58.
[27]J. U. Andersen and E. Uggerhøj, Can. J. Phys. 46, 517 (1968).
[28]H. A. Fowler and C. Erginsoy, Phys. Letters 24A, 390 (1967).
[29]J. H. Barrett, Phys. Rev. 166, 219 (1968).
[30]Some recent measurements in Linchard's low-energy range and references to earlier such measurements are reported by I. A. Abroyan, V. A. Koryukin, N. N. Ushakov, and L. A. Tseknovicher, Fiz. Tverd. Tela 11, 3376 (1969) [Soviet Phys. Solid State 11, 2745 (1970)].
[31]J. U. Andersen and L. C. Feldman, Phys. Rev. B 1, 2063 (1970).
[32]D. V. Morgan and D. Van Vliet, Can. J. Phys. 46, 503 (1968).
[33]D. V. Morgan and D. Van Vliet, Ref. 6, p. 476.
[34]T. S. Noggle and J. H. Barrett, Phys. Status Solidi 36, 761 (1969).
[35]Reference 29. The value of ψ_b for the vibrating plane quoted there is slightly smaller than the value given here because a was calculated in the earlier paper from Eq. (3b), whereas (3a) was used for the results given here.
[36]G. Foti, F. Grasso, and E. Rimini, Nuovo Cimento Letters 1, 941 (1969).
[37]J. U. Andersen, J. A. Davies, K. O. Nielsen, and S. L. Andersen, Nucl. Instr. Methods 38, 210 (1965).
[38]E. Bøgh and E. Uggerhøj, Nucl. Instr. Methods 38, 216 (1965).
[39]B. Domeij and K. Bjorkqvist, Phys. Letters 14, 127 (1965).
[40]B. R. Appleton, Sheldon Datz, C. D. Moak, and Mark T. Robinson (unpublished).
[41]E. Bøgh, Phys. Rev. Letters 19, 61 (1967).
[42]B. R. Appleton and L. C. Feldman, Ref. 6, p. 417.
[43]The fact that the straight-line fit passes through the origin within the error limits of the calculation should not be taken to imply that $\chi = 0$ for $u_2^2 = 0$. The significant portion of the fit is for the physically realizable range of u_2^2: 10^{-3} Å^2 and above.
[44]J. A. Davies, L. Eriksson, N. G. E. Johansson, and I. V. Mitchell, Phys. Rev. 181, 548 (1969); M. R. Altman, L. C. Feldman, and W. M. Gibson, Phys. Rev. Letters 24, 464 (1970).
[45]V. S. Kulikauskas, M. M. Malov, and A. F. Tulinov, Zh. Eksperim. i Teor. Fiz. 53, 487 (1968) [Soviet Phys. JETP 26, 321 (1968)].
[46]E. Bøgh, Can. J. Phys. 46, 653 (1968).
[47]L. C. Feldman and B. R. Appleton, Appl. Phys. Letters 15, 305 (1969).
[48]E. Bøgh and J. L. Whitton, Phys. Rev. Letters 19, 553 (1967).
[49]E. Bøgh, Ref. 5, p. 76.
[50]B. R. Appleton and L. C. Feldman (private communication).
[51]C. Erginsoy, Phys. Rev. Letters 15, 360 (1965).
[52]B. R. Appleton, C. Erginsoy, and W. M. Gibson, Phys. Rev. 161, 330 (1967).

PHYSICAL REVIEW B VOLUME 3, NUMBER 5 1 MARCH 1971

Alpher-Rubin Ultrasonic Attenuation and Dipolar Nuclear-Acoustic-Resonance Coupling in Pure Metals*

J. G. Miller, W. D. Smith,† D. I. Bolef, and R. K. Sundfors
Arthur Holly Compton Laboratory of Physics, Washington University, Saint Louis, Missouri 63130
(Received 27 August 1970)

Experimental results are presented of measurements of the very small magnetic-field-dependent changes in the attenuation $\Delta\alpha$ of ultrasound (absorptive Alpher-Rubin effect) in pure single crystals of Al, Cu, Nb, and Ta. Measurements were made at 293 K in magnetic fields ranging from 0 to 11 kOe, using both longitudinal and transverse acoustic waves. Variations of $\Delta\alpha$ with both orientation and magnitude of the external magnetic field were studied. Measurements of the dependence of $\Delta\alpha$ on frequency over the range 5–250 MHz were made. The results are particularly relevant to the study of induced dipolar coupling in nuclear acoustic resonance. A derivation is given of expressions for the nuclear-acoustic-resonance signal in pure metals.

I. INTRODUCTION

The influence of a magnetic field on the propagation of acoustic waves in solid metals was first considered theoretically by Alpher and Rubin.[1] The Alpher-Rubin phenomenological theory predicts changes in both the acoustic phase velocity (dispersion) and the acoustic attenuation (absorption) when a static magnetic field is applied. Galkin and Koroliuk[2] verified the predicted dependence of acoustic velocity on the magnitude of the magnetic field for longitudinal acoustic waves propagating in polycrystalline tin and aluminum. In a comprehensive study, Alers and Fleury[3] verified the predicted dependence of acoustic velocity on both magnitude and orientation of an external field for longitudinal and transverse 10-MHz acoustic waves. A review of the dispersive Alpher-Rubin effect has been given by Alers.[4]

The magnetic field dependence of the acoustic at-

tenuation predicted by Alpher and Rubin was observed first by Shapira and Neuringer[5] at 77 K in low-conductivity alloys using high magnetic fields. So small are the field-dependent attenuation changes $\Delta\alpha$ that they have been observed, until the present work, only with very high magnetic fields and, with one exception,[6] in high-resistivity alloys. A review of much of this work has been given by Shapira.[7]

The interaction which gives rise to the Alpher-Rubin effect also serves as a coupling mechanism between the magnetic dipole moments of the nuclear spin system and the ultrasonic waves. In this paper we present results of measurements of the absorptive Alpher-Rubin effect in single crystals of pure Al, Cu, Nb, and Ta in magnetic fields up to 11 kOe. The results, because of the choice of pure metals and relatively low magnetic fields, are particularly relevant to the newly opened field of nuclear acoustic resonance (NAR) in single-crystal metals.[8-12] From the formalism which leads to the theory of the Alpher-Rubin effect, expressions are derived which account for the NAR signal in pure metals.

Measurements were made using both pulse-echo and continuous-wave (cw) techniques, the latter by the use of a continuous-wave marginal oscillator ultrasonic spectrometer (MOUS) operating in either the conventional or the self-modulated mode.[13] (A preliminary report of part of the present work was given in Ref. 13.) Longitudinal and transverse acoustic waves at 293 K were utilized. In addition to measurements of the dependence of $\Delta\alpha$ on magnitude and orientation of magnetic field, measurements of the frequency dependence were made between 5 and 250 MHz. The frequency dependence of the Alpher-Rubin effect has not previously been measured. To demonstrate the usefulness of the sensitive cw technique used in the present work, measurements were also made of the dispersive Alpher-Rubin effect in aluminum.

We present in Sec. II of this paper a summary of the classical theory of the interaction giving rise to both the Alpher-Rubin effect and the dipolar coupled NAR in metals. In Sec. III, a brief description is given of the cw and pulsed ultrasonic techniques used in the measurements. The experimental results on the Alpher-Rubin effect and a comparison between theory and experiment are presented in Sec. IV. In Sec. V, expressions for the dipolar coupled NAR signal are given and the relevance of the present results to NAR measurements is discussed.

II. THEORY

In this section we review the Alpher and Rubin[1] phenomenological treatment of the propagation of an ultrasonic wave in a metallic solid in the presence of an applied magnetic field. The theory accounts for the electromagnetic fields generated by the ultrasonic wave as well as the changes in ultrasonic phase velocity and attenuation arising from the coupling to the charge-carrier system. Several microscopic treatments[14-20] of the interaction have been presented which expand upon and delineate the range of validity of the Alpher-Rubin theory. The present work was carried out in a range of frequencies and temperatures for which the phenomenological treatment is applicable.

We consider a small-amplitude elastic plane wave propagating in the x direction with phase velocity v_0. A static magnetic field $\vec{H}_0$ is applied at an arbitrary angle to the direction of propagation. We assume that the electron-lattice coupling is sufficiently strong that we may consider the Lorentz force to be acting directly on the lattice. Under these assumptions, the equation of motion for the ionic displacement $\vec{\xi}$ is

$$\frac{\partial^2\vec{\xi}}{\partial t^2} = v_0^2\,\frac{\partial^2\vec{\xi}}{\partial x^2} + \frac{\mu}{c\rho}\,[\vec{j}\times(\vec{H}_0+\vec{h})], \tag{1}$$

where $\vec{j}$ is the induced current density, $\vec{h}$ the induced rf magnetic field associated with the ultrasonic wave, μ the permeability, c the velocity of light, and ρ the mass density. The microscopic theory of Rodriguez demonstrates that the assumption that the Lorentz force acts directly on the lattice is justified if $\omega\tau$, kl, and $\omega_c\tau \ll 1$. Here τ is the mean scattering time for electrons, l the electron mean free path, and ω_c the cyclotron frequency. These conditions require that the conduction electrons attain momentum equilibrium with the lattice in times and distances which are short compared to the period and wavelength, respectively, of the ultrasonic wave. At 300 K in pure metals $\tau \sim 10^{-14}$ sec, $l \sim 10^{-5}$–10^{-6} cm, and $\omega_c \sim 10^{11}$ Hz for 100 kOe. The phenomenological[1] theory thus applies to the case of pure metals at 300 K for frequencies below 300 MHz and fields under 100 kOe. The current density is

$$\vec{j} = \sigma\vec{e} + \frac{\sigma\mu}{c}\left(\frac{\partial\vec{\xi}}{\partial t}\times(\vec{H}_0+\vec{h})\right), \tag{2}$$

where $\vec{e}$ is the rf electric field and σ the dc conductivity. The two Maxwell equations used in this treatment may be written in the form

$$\nabla\times\vec{e} = -\frac{\mu}{c}\,\frac{\partial(\vec{H}_0+\vec{h})}{\partial t}, \tag{3}$$

$$\nabla\times(\vec{H}_0+\vec{h}) = \frac{4\pi}{c}\,\vec{j} + \frac{\epsilon}{c}\,\frac{\partial\vec{e}}{\partial t}, \tag{4}$$

where ϵ is the permittivity. Since the induced quantities $\vec{e}$, $\vec{h}$, and $\vec{j}$ are assumed to be associated with the lattice displacement $\vec{\xi}$, all these quantities are taken to be proportional to $e^{i(\omega t - kx)}$.

Equations (1) and (4) may be combined to yield

$$\frac{\partial^2\vec{\xi}}{\partial t^2} = v_0^2\,\frac{\partial^2\vec{\xi}}{\partial x^2} - \frac{\mu\epsilon}{4\pi\rho c}\left(\frac{\partial\vec{e}}{\partial t}\times(\vec{H}_0+\vec{h})\right)$$

$$+\frac{\mu}{4\pi\rho}\left[\nabla\times(\vec{H}_0+\vec{h})\times(\vec{H}_0+\vec{h})\right] . \tag{5}$$

The components of $\vec{e}$ and $\vec{h}$ are obtained from the current density and the two Maxwell equations. Once the vector components of the self-consistent electromagnetic fields are known for a particular polarization of the ultrasonic wave, Eq. (5) leads to a dispersion relationship. From that relationship are obtained the changes in the ultrasonic phase velocity and attenuation due to the static magnetic field. A detailed derivation is presented elsewhere.[21] Of interest here are (i) the values of the local magnetic field $\vec{h}$ which couples to the nuclear dipole moment in NAR, and (ii) the changes in acoustic phase velocity and attenuation associated with the Alpher-Rubin interaction. We choose our coordinate system (Fig. 1) so that $\vec{H}_0$ is in the $\hat{x}$-$\hat{z}$ plane making an angle θ with $\hat{x}$ axis. The induced magnetic field and the changes in phase velocity and attenuation for a longitudinal wave ($\vec{\xi}=\xi_x\hat{x}$) are found to be

$$\vec{h}\cong-\epsilon_{xx}\frac{1+i\beta_l}{1+\beta_l^2}H_0\sin\theta\,\hat{z} , \tag{6}$$

$$\Delta\alpha\cong\frac{\sigma\mu^2}{2\rho v_{l0}c^2}\frac{\beta_l^2}{1+\beta_l^2}H_0^2\sin^2\theta , \tag{7}$$

$$\frac{\Delta v_l}{v_{l0}}\cong\frac{\mu}{8\pi\rho v_{l0}^2}\frac{1}{1+\beta_l^2}H_0^2\sin^2\theta , \tag{8}$$

where the phase-shift parameter $\beta_l=\omega c^2/4\pi\mu\sigma v_{l0}^2$, and $\epsilon_{xx}=\partial\xi_x/\partial x$. A transverse wave with arbitrary polarization in the y-z plane ($\vec{\xi}=\xi_y\hat{y}+\xi_z\hat{z}$) results in

$$\vec{h}=\epsilon_{yx}\frac{1+i\beta_t}{1+\beta_t^2}H_0\cos\theta\,\hat{y} + \epsilon_{zx}\frac{1+i\beta_t}{1+\beta_t^2}H_0\cos\theta\,\hat{z} , \tag{9}$$

$$\Delta\alpha=\frac{\sigma\mu}{2\rho v_{t0}c^2}\frac{\beta_t^2}{1+\beta_t^2}H_0^2\cos^2\theta , \tag{10}$$

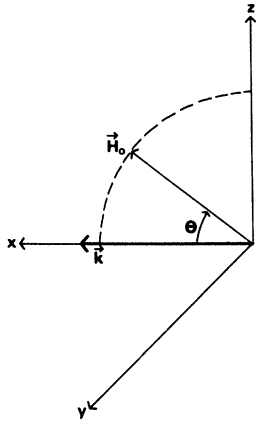

FIG. 1. Orientation of acoustic wave propagation vector $\vec{k}$ and magnetic field $\vec{H}_0$ in a coordinate system fixed relative to the crystal axes. $\vec{H}_0$ rotates in the xz plane.

$$\frac{\Delta v_t}{v_{t0}}=\frac{\mu}{8\pi\rho v_{t0}^2}\frac{1}{1+\beta_t^2}H_0^2\cos^2\theta , \tag{11}$$

where $\beta_t=\omega c^2/4\pi\mu\sigma v_{t0}^2$, $\epsilon_{yx}=\partial\xi_y/\partial x$, and $\epsilon_{zx}=\partial\xi_z/\partial x$. The induced $\vec{e}$ fields are negligible; their magnitudes are down from those of the $\vec{h}$ fields by factors of the order of v/c. Terms of the order of $\mu H_0^2/4\pi\rho v_0^2$ have been dropped as negligible compared to unity in Eqs. (7), (8), (10), and (11).

The $\vec{h}$ fields and their relationship to NAR in metals are discussed in Sec. V. In connection with the experimental results presented in Sec. IV, $\Delta\alpha$ and $\Delta v/v$ are discussed in detail. We note that the frequency dependence of $\Delta\alpha$ is contained in the term $\beta^2/(1+\beta^2)$, and that of $\Delta v/v_0$ in the term $1/(1+\beta^2)$. For sufficiently low frequencies ($\beta^2\ll1$), $\Delta\alpha$ varies as ω^2 while $\Delta v/v_0$ is frequency independent. At frequencies for which $\beta^2\gg1$, $\Delta\alpha$ is essentially frequency independent, while $\Delta v/v_0$ varies as ω^{-2}. For low-conductivity metals, or for low acoustic velocities, β^2 can be large compared to 1 at relatively low frequencies. For 20-MHz transverse waves propagating in a $\langle110\rangle$ direction with a $\langle\bar{1}10\rangle$ polarization, for example, $\beta_t^2\simeq0.42$ for copper and $\beta_t^2\simeq8.9$ for vanadium.

III. EXPERIMENTAL PROCEDURE

Of the four single-crystal specimens studied in the present experiment, the Al crystal was obtained from Alfa Crystals, the Cu, Nb, and Ta crystals from the Westinghouse Lamp Division, Bloomfield, N. J. The impurity content of the Al and Cu crystals, provided by the suppliers, was less than 100 ppm by weight. The resistivity ratios of the Nb and Ta crystals were both $\simeq200$. All four crystals were in the form of cylinders. The cylindrical axes of the Al, Cu, and Ta crystals were oriented along the [110] crystallographic axis, that of the Nb crystal along the [111] axis. Dimensions of the crystals were Al, 0.75 in. diam × 0.625 in. length; Cu, 1.00 in. diam × 0.50 in. length; Nb and Ta, 0.25 in. diam × 0.40 in. length. After suitable etching to remove damage resulting from cutting, the end faces of all four crystals were ground and polished to a flatness of 50×10^{-6} in. (for Al and Cu) and 10×10^{-6} in. (for Nb and Ta) and a parallelism of 30 sec of arc (for Al and Cu) and 10 sec of arc (for Nb and Ta). The crystals were oriented to $\pm1^\circ$ by means of standard Laue x-ray back-reflection techniques.

Standard AT- and X-cut quartz transducers were used in a reflection scheme to generate transverse and longitudinal waves, respectively. Nonaq vacuum grease was used as the acoustic bond. Magnetic field measurements, utilizing a Harvey-Wells (Magnion) 12-in. regulated electromagnet, were ac-

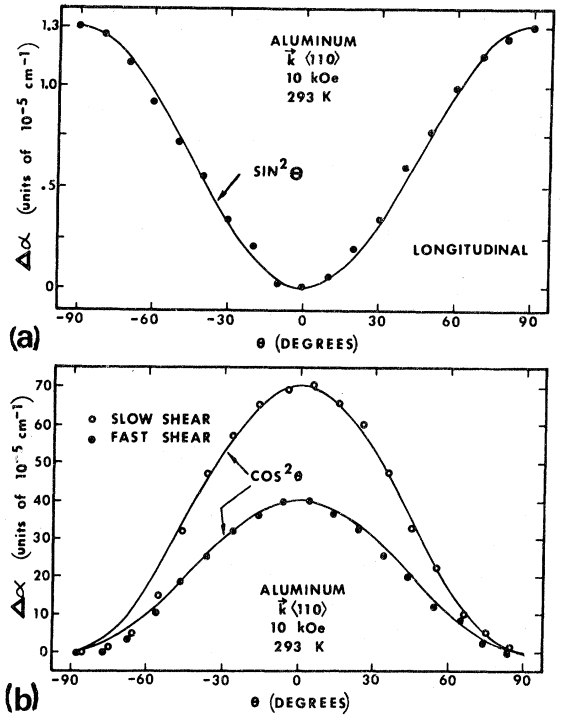

FIG. 2. Increase in attenuation as a function of magnet angle θ in Al [110] at $H = 10$ kOe for (a) 10-MHz longitudinal waves, and (b) 10-MHz transverse waves. Theoretical $\sin^2\theta$ and $\cos^2\theta$ have been fitted to the data (solid lines).

curate to ± 1 Oe in magnitude and to ± 1° in orientation.

Measurements of $\Delta\alpha$ and $\Delta v/v$ were made using both cw and pulse-echo ultrasonic techniques. The MOUS, previously used only in NAR studies, has been applied recently to the study of nonresonant attenuation and velocity changes.[13,22,23] A detailed description of the modes of operation of the MOUS is given in Ref. 13. In the present work, the MOUS was operated in the conventional mode for velocity measurements and in the self-modulated mode using either the rms or frequency pulling technique for attenuation measurements. In the latter mode, the spectrometer provides an output proportional to $\Delta\alpha$. The absolute magnitude of the attenuation change in the self-modulated mode was determined directly by monitoring the oscillator rf voltage while the effective resistances of the acoustic probe and calibrator were changed. Details of the calibration procedure have been described elsewhere.[21] Operated in the conventional mode, the marginal oscillator "tracks" the frequency of a mechanical resonance. Changes in velocity thus result in changes in the oscillator frequency which were monitored by means of a frequency counter. Using the MOUS, attenuation changes as small as 10^{-6} cm^{-1} were observed; changes of $\Delta v/v$ of 10^{-7} were detected. For the frequency-dependent measurements, a commercial pulse-echo spectrometer (Matec, Inc.) was used. By use of the automatic attenuation recorder of this spectrometer, changes in attenuation of the order of 10^{-4}–10^{-5} cm^{-1} were measured.

IV. EXPERIMENTAL RESULTS AND DISCUSSION

We present the experimental results of measurements of the Alpher-Rubin absorptive effect in pure Al, Cu, Nb, and Ta in two parts: the dependence of $\Delta\alpha$ on θ and H, and the dependence of $\Delta\alpha$ on frequency. Results of the application of the cw technique to the measurement of the dispersive Alpher-Rubin effect in Al are also presented. All measurements were carried out at room temperature (~ 293 K).

A. Dependence of $\Delta\alpha$ on θ and H

The dependence of $\Delta\alpha$ on angle θ between $\vec{H}$ and $\vec{k}$ and on the magnetic field magnitude H was measured on the single crystals of aluminum, copper, and tantalum for several of the three pure modes of acoustic wave propagation in the [110] direction, i.e., waves polarized along the [110] (longitudinal), the [001] ("fast shear"), and the [$\bar{1}$10] ("slow shear") directions. For single crystal Nb, the analogous measurements were made for longitudinal waves propagated along the [111] axis. In all cases agreement between theory and experiment was excellent. Representative cases are shown in Figs. 2 and 3. In Fig. 2 are shown the measured dependences of $\Delta\alpha$ on angle θ at 10 kOe and 293 K in pure aluminum for longitudinal waves [Fig. 2(a)] and for transverse waves polarized along the [001] and [$\bar{1}$10] crystal axes [Fig. 2(b)]. The theoretically expected $\sin^2\theta$ (longitudinal) and $\cos^2\theta$ (transverse) dependences are shown by the solid curve. The calculated and experimental values of $\Delta\alpha$ agree to within a few percent. The values of the crystal parameters used in calculating absolute values of $\Delta\alpha$ are given in Table I. Analogous results, for pulse-echo measurements with 15-MHz longitudinal waves in single-crystal Nb, are shown in Fig. 3(a) ($\Delta\alpha$ as a function of H^2) and Fig. 3(b) ($\Delta\alpha$ as a function of θ). The value of σ(Nb) given in Table I was obtained by matching a best straight line to the data of Fig. 3(a). The theoretical curve (solid line) in Fig. 3(b) was then obtained from Eq. (7), using the calculated value of σ and the constants given in Table I, with no adjustable parameters. The results for $\Delta\alpha$ vs H^2 and θ in Cu and Ta (not shown) also demonstrated excellent agreement between theory and experiment.

As discussed briefly in Sec. III, the MOUS, when operated in the conventional single-frequency mode and without modulation, is especially well adapted to the measurement of small changes ($\Delta v/v \simeq 10^{-7}$)

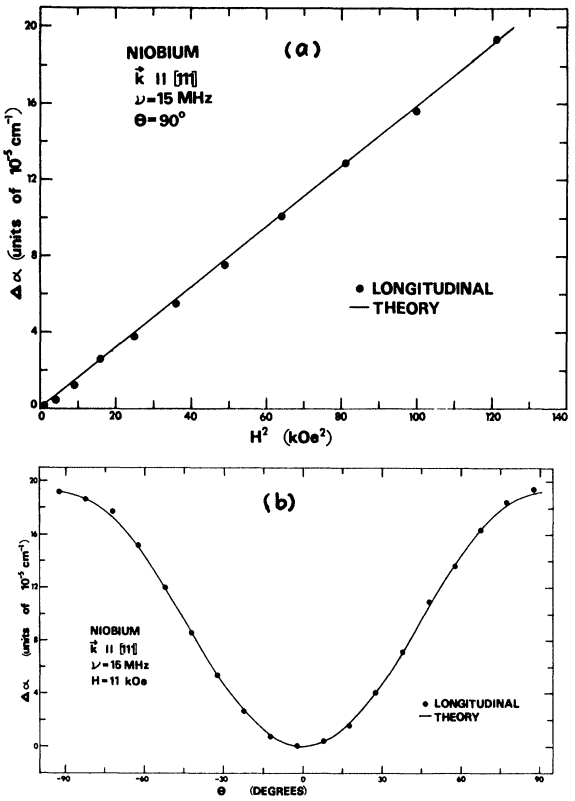

FIG. 3. Increase in attenuation in Nb [111] for 15-MHz longitudinal waves: (a) as a function of H^2 – solid line is a straight-line fit to the data; (b) as a function of magnet angle θ – solid curve corresponds to the values calculated from Eq. (7), using σ as obtained from the data of (a).

in ultrasonic velocity. As a check on the attenuation results, the dependence on magnetic field angle and magnitude of the velocity changes was measured. For longitudinal waves along a ⟨110⟩ axis in aluminum, from Eq. (8) one obtains $\Delta v_l/v_l = 3.5\times10^{-6}$ for an applied field of 10 kOe. Experimentally, a change of 35 ± 1 Hz in 10 MHz was observed, in excellent agreement with the theory. (The ± 1 uncertainty is inherent in the frequency-counting technique and does not reflect an inaccuracy in the marginal oscillator measurement technique.) Similar good agreement with theory for the velocity data was reported by Alers and Fleury.[3,4]

B. Dependence of $\Delta\alpha$ on Frequency

The frequency dependence of $\Delta\alpha$ for longitudinal and transverse acoustic waves in aluminum is shown in Fig. 4. The magnitude of the applied magnetic field was 11 kOe. The orientation was chosen [θ (longitudinal) = 90°, θ (transverse) = 0°] to maximize the angular factor for each polarization. The analogous data of $\Delta\alpha$ for transverse waves in copper is shown in Fig. 5 for $H = 11$ kOe, $\theta = 0°$.

TABLE I. Crystal parameters used in calculating absolute values of $\Delta\alpha$ and $\Delta v/v$ at ~293 K.

Metal	ρ (g/cm³)	$\hat{k}$	$\hat{\xi}$	v (10^5 cm/sec)	σ (10^6 mho/cm)
Al	2.70	[110]	[110]	6.35	0.354
			[001]	3.27	
			[$\bar{1}$10]	2.92	
Cu	8.92	[110]	[110]	4.97	0.591
			[001]	2.91	
			[$\bar{1}$10]	1.62	
Nb	8.58	[111]	[111]	4.84	0.062
Ta	16.68	[110]	[110]	4.22	0.064
			[001]	2.22	
			[$\bar{1}$10]	1.78	

As remarked in Sec. II, the frequency dependence of $\Delta\alpha$ is contained in the factor $\beta^2/(1+\beta^2)$ [see Eqs. (7) and (10)]. Values of the phase-shift parameter β at 10, 20, and 100 MHz for a number of metals are given in Table II. The calculated curves of $\Delta\alpha$ as a function of frequency are shown as solid lines in Figs. 4 and 5. In none of the cases shown

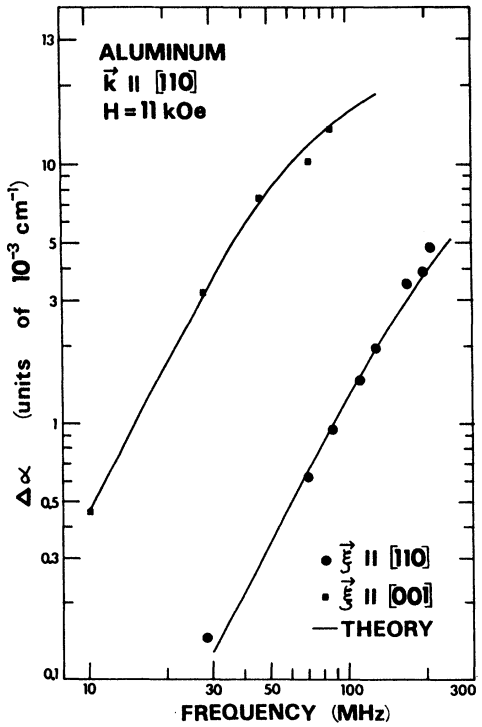

FIG. 4. Increase in attenuation as a function of frequency in Al [110] at $H = 11$ kOe for longitudinal and transverse ($\vec{\xi} \parallel [001]$) waves. Solid lines represent values calculated from Eqs. (7) and (10).

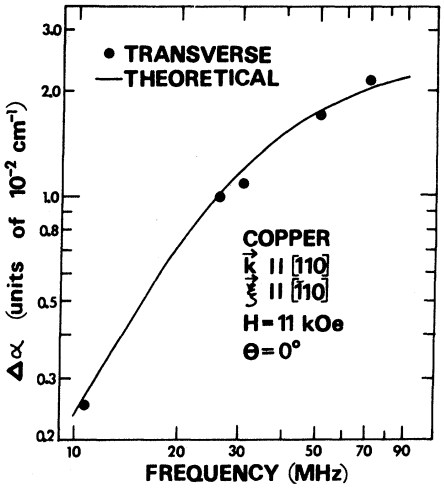

FIG. 5. Increase in attenuation as a function of frequency in Cu [110] at $H = 11$ kOe for transverse waves. Solid lines correspond to theoretical predictions.

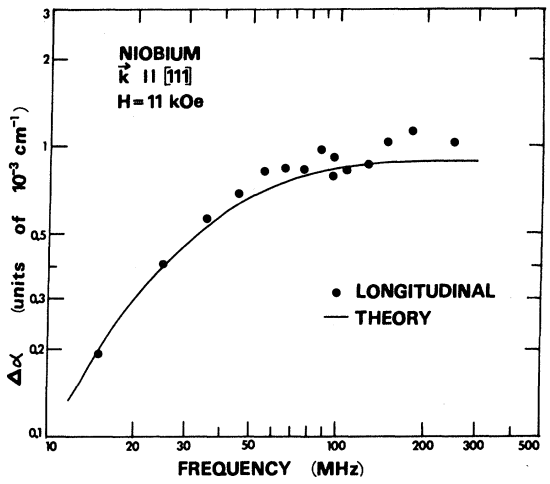

FIG. 6. Increase in attenuation as a function of frequency in Nb [111] at $H = 11$ kOe for longitudinal waves. Solid lines correspond to theoretical predictions.

for Al and Cu is the condition $\beta^2 \gg 1$ achieved, although for transverse ("slow-shear") waves in Cu (Fig. 5) a noticeable decrease in slope of the $\Delta\alpha$ vs ν curve is evident at 50 MHz and above.

In Figs. 6 and 7, finally, are shown the dependence on frequency of $\Delta\alpha$ for the single crystals of Nb and Ta described in Sec. III. The relatively low values of conductivity (compared with those for Al and Cu above) are reflected in a larger value of β at a given frequency, resulting in a marked decrease in slope of the $\Delta\alpha$-vs-ν curve for longitudinal waves in Nb and Ta above 50 MHz, and for transverse waves in Ta above 15 MHz. The theoretical (absolute) values of $\Delta\alpha$, calculated using the values of the parameters given in Table I, are shown as solid lines in Figs. 6 and 7. Agreement between theory and experiment is seen to be better for the case of longitudinal than for transverse waves. This discrepancy may be explained in part by the increasingly poorer signal-to-noise ratio as one progressed from v_l to $v_t(\vec{\xi}[001])$ to v_t $(\vec{\xi}[\bar{1}10])$. The relevance for NAR of the frequency dependence of the interaction and the significance of the phase-shift factor β is discussed in Sec. V.

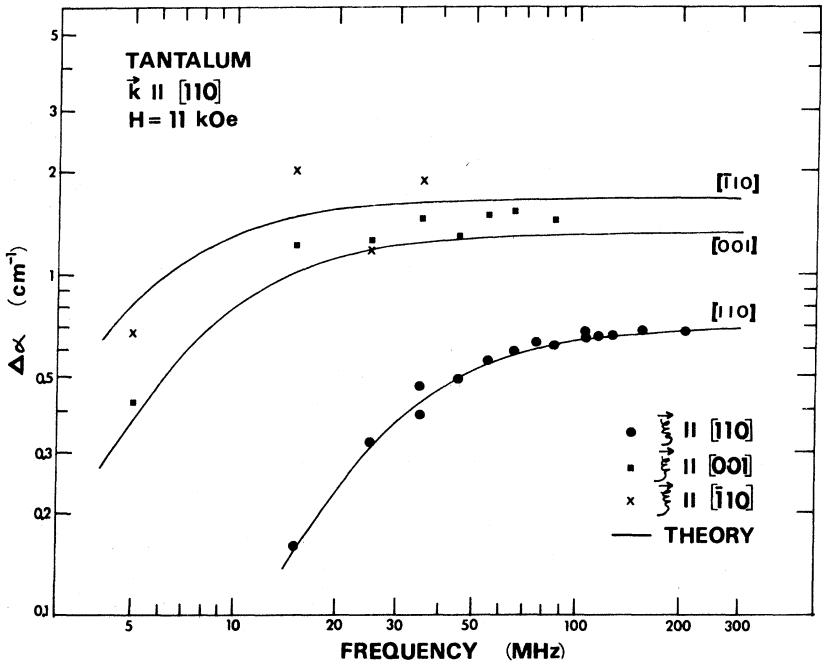

FIG. 7. Increase in attenuation as a function of frequency in Ta [110] at $H = 11$ kOe for longitudinal and transverse waves. Solid lines correspond to theoretical predictions.

TABLE II. Values of the phase shift parameter β for selected metals at 10, 20, and 100 MHz and at 77 and 300 K.

Metal	ρ (g/cm^3)	$\hat{k}$	$\hat{\xi}$	v (10^5 cm/sec)	σ (10^6 mho/cm) 77 K	σ (10^6 mho/cm) 300 K	β 10 MHz 77 K	β 10 MHz 300 K	β 20 MHz 77 K	β 20 MHz 300 K	β 100 MHz 77 K	β 100 MHz 300 K
Al	2.70[a]	[110]	[110]	6.35[b]	4.52[c]	0.354[d]	0.003	0.035	0.006	0.070	0.028	0.351
			[001]	3.27			0.010	0.132	0.021	0.264	0.104	1.323
			[$\bar{1}$10]	2.92			0.013	0.166	0.026	0.332	0.130	1.658
Cu	8.92[e]	[110]	[110]	4.97[d]	5.21[c]	0.591[d]	0.004	0.034	0.008	0.069	0.039	0.344
			[001]	2.91			0.011	0.100	0.022	0.200	0.114	1.00
			[$\bar{1}$10]	1.62			0.037	0.322	0.073	0.644	0.366	3.22
Ag	10.51[a]	[110]	[110]	3.42[f]	3.62[c]	0.682[d]	0.012	0.063	0.024	0.126	0.118	0.628
			[001]	2.07			0.032	0.172	0.065	0.343	0.323	1.715
			[$\bar{1}$10]	1.25			0.088	0.468	0.177	0.936	0.883	4.68
Au	17.0[a]	[110]	[110]	3.47[d]	2.23[c]	0.41[d]	0.064	0.108	0.128	0.216	0.639	1.079
			[001]	1.47			0.100	0.565	0.200	1.130	0.998	5.65
			[$\bar{1}$10]	0.87			0.284	1.610	0.568	3.22	2.84	16.12
V	6.02[e]	[110]	[110]	6.00[e]	0.385[g]	0.04[d]	0.036	0.348	0.072	0.696	0.361	3.48
			[001]	2.68			0.182	1.749	0.363	3.500	1.816	17.49
			[$\bar{1}$10]	3.02			0.143	1.375	0.286	2.750	1.43	13.75
Nb	8.58[e]	[110]	[110]	5.05[e]	0.338[c]	0.062[g]	0.058	0.316	0.116	0.632	0.580	3.16
			[001]	1.83			0.443	2.41	0.886	4.81	4.43	24.1
			[$\bar{1}$10]	2.56			0.225	1.276	0.450	2.55	2.25	12.76
Ta	16.68[e]	[110]	[110]	4.22[e]	0.396[c]	0.064[d]	0.071	0.440	0.142	0.880	0.711	4.40
			[001]	2.22			0.256	1.581	0.512	3.16	2.56	15.81
			[$\bar{1}$10]	1.78			0.400	2.48	0.800	4.96	4.00	24.8
Re	20.53[a]	[010]	[010]	5.49[f]	0.400[g]	0.0518[a]	0.042	0.321	0.083	0.642	0.415	3.21
			[001]	2.80			0.160	1.232	0.320	2.464	1.598	12.32
			[210]	2.88			0.151	1.166	0.302	2.332	1.509	11.66
Pt	21.45[a]	[110]	[110]	3.89[f]	0.520[c]	0.0943[a]	0.064	0.351	0.127	0.702	0.636	3.51
			[001]	1.89			0.270	1.487	0.540	2.97	2.70	14.87
			[$\bar{1}$10]	1.50			0.430	2.37	0.860	4.74	4.30	23.7
Tl	11.85[a]	[010]	[010]	1.88[f]	0.278[g]	0.556[a]	0.510	2.55	1.020	5.10	5.10	25.5
			[001]	0.779			2.96	14.83	5.92	29.6	29.6	148.3
			[210]	0.473			8.05	40.3	16.10	80.6	80.5	403
Pb	11.34[a]	[110]	[110]	2.06[b]	0.201[g]	0.0484[a]	1.858	2.44	3.72	4.88	18.58	24.4
			[001]	1.13			1.936	8.05	3.87	16.10	19.36	80.5
			[110]	0.567			7.75	32.1	15.50	64.2	77.5	321

[a] *Handbook of Chemistry and Physics*, 48th ed. (Chemical Rubber, Cleveland, Ohio, 1967).
[b] Landolt-Börnstein (Springer-Verlag, Berlin, 1966), Group III, Vol. 1.
[c] Natl. Bur. Std. Technical Note 365, 1968 (unpublished).
[e] D. I. Bolef, J. Appl. Phys. 32, 100 (1961).
[f] Landolt-Börnstein (Springer-Verlag, Berlin, 1969), Group III, Vol. 2.
[g] G. T. Meaden, *Electrical Resistance of Metals*, (Plenum, New York, 1965), p. 15, Table II.

V. MAGNETIC DIPOLAR COUPLING IN NAR

Ultrasonically induced nuclear spin resonance has been reported in tantalum, niobium, rhenium, aluminum, and vanadium. The interaction mechanism in Ta,[8,9] Nb,[24] and Re[11] is thought to be the well-known coupling between the electric quadrupole moment of the nucleus and the oscillating electric field gradient produced by the ultrasonic wave. Evidence[10,12] indicates that the mechanism in Al and V is the coupling between the nuclear dipole moment and the oscillating magnetic field [Eq. (6) or (9)] induced by the ultrasonic wave in the presence of an applied magnetic field. A preliminary calculation[10] of the ultrasonic attenuation α_n arising from the NAR has been carried out under

the assumption that $\beta = 0$. The experimental results are in good agreement with the calculated angular dependence and, within the limits of experimental accuracy, are not inconsistent with the calculated ω^4 frequency dependence. In this section we generalize the calculation of the NAR attenuation to include $\beta \neq 0$. The present treatment predicts quantitatively the observed line shape which represents a mixture of the absorptive and dispersive components of the magnetic susceptibility. The ω^4 frequency dependence is found to apply only in a low-frequency limit discussed below.

The component of the ultrasonically induced rf magnetic field perpendicular to the applied magnetic field $\vec{H}_0$ is thought to be responsible for inudcing the NAR. From Eq. (6) or (9), it is clear that an ultrasonic wave varying as $\cos\omega t$ results in an induced magnetic field h_1 perpendicular to H_0 which contains a component oscillating 90° out of phase with the ultrasonic wave,

$$h_1 = h_1' \cos\omega t - h_1'' \sin\omega t .$$

In terms of a macroscopic vector model[25] an oscillating magnetic field $\vec{h}_1$ results in a magnetization

$$\vec{M} = \chi \vec{h}_1 = (\chi' - i\chi'')\vec{h}_1$$

in the direction of the oscillating magnetic field, where χ' and χ'' are the components of the magnetic susceptibility. In the present case, therefore, we obtain for the resulting magnetization

$$M = (\chi' h_1' + \chi'' h_1'') \cos\omega t + (\chi'' h_1' - \chi' h_1'') \sin\omega t . \quad (12)$$

The magnitude of the power $|\bar{P}|$ absorbed by the spin system is

$$\langle -M dh_1/dt \rangle_{\text{av}} = \tfrac{1}{2}\omega (h_1')^2 \left[1 + \left(\frac{h_1''}{h_1'}\right)^2\right] \chi'' ,$$

where the average is with respect to time. The NAR measurements in aluminum and vanadium were made using a MOUS, however, which responds[13] not to the magnitude of the power absorbed by the spin system but to the component $\bar{P}_{\text{MOUS}}$ of the power associated with that part of the magnetization in phase with $(d/dt)(h_1' \cos\omega t)$. That is,

$$\bar{P}_{\text{MOUS}} = \left\langle -M \frac{d}{dt} (h_1' \cos\omega t) \right\rangle_{\text{av}}$$

or

$$\bar{P}_{\text{MOUS}} = \tfrac{1}{2}\omega (h_1')^2 [\chi'' - (h_1''/h_1')\chi'] . \quad (13)$$

The presence of an out-of-phase component h_1'' of the oscillating magnetic field thus results in a marginal-oscillator output containing a mixture of the absorptive and dispersive components of the magnetic susceptibility.

From Eq. (6) or (9), the component

$$h_1 = h_1' \cos\omega t - h_1'' \sin\omega t$$

of h perpendicular to H_0 is given by

$$h_1 = \frac{\epsilon H_0 f(\theta)}{1+\beta^2} (\cos\omega t - \beta \sin\omega t), \quad (14)$$

where $\epsilon = \epsilon_{xx'}$, $\epsilon_{yx'}$, or ϵ_{zx} and $f(\theta)$ and β are determined by the polarization of the ultrasonic wave. For longitudinal waves ($\epsilon_{xx} \neq 0$), h_1 is proportional to $f(\theta) = \sin\theta \cos\theta$. For transverse waves with particle motion ($\epsilon_{zx} \neq 0$) in the plane defined by $\vec{k}$ and $\vec{H}_0$, $f(\theta) = \cos^2\theta$. For transverse waves with particle motion ($\epsilon_{yx} \neq 0$) perpendicular to that plane, the factor is $f(\theta) = \cos\theta$.

Using Eq. (14), one can write $h_1''/h_1' = \beta$ and

$$h_1' = h_{10}' \cos\omega t/(1+\beta^2),$$

where $h_{10}' = \epsilon H_0 f(\theta)$. The expression for the average power absorbed by the spin system is then given by

$$\bar{P} = \tfrac{1}{2}\omega (h_{10}')^2 \chi'' [1/(1+\beta^2)], \quad (15)$$

and $\bar{P}_{\text{MOUS}}$ by

$$\bar{P}_{\text{MOUS}} = \tfrac{1}{2}\omega (h_{10}')^2 [(\chi'' - \beta\chi')/(1+\beta^2)^2] . \quad (16)$$

Whereas $\bar{P}_{\text{MOUS}}$ corresponds to the acoustic power absorbed by the nuclear spins when the MOUS is used, $\bar{P}$ corresponds to the power absorbed when certain pulse-echo ultrasonic spectrometers[26] or transmission ultrasonic spectrometers[27,28] are used. At present, because of the stringent sensitivity requirements imposed by the very weak signals, NAR in metals has been seen only with MOUS.

The ultrasonic (amplitude) attenuation α_n as a result of the nuclear spin resonance is given by the relationship $\alpha_n = \frac{1}{2}P/P_0$, where P_0 is the acoustic power per unit area introduced into the crystal.[29] Restricting the treatment to cases of longitudinal or transverse waves propagating along the [100] or [110] axis in cubic crystals, we have $P_0 = \frac{1}{2}\rho v^3 \epsilon^2$. Combining these expressions with Eqs. (13) and (14) results in the desired expression for α_n. In order for the frequency dependence of the interaction to appear explicitly in α_n, we write $H_0 = \omega/\gamma$, where γ is the nuclear gyromagnetic ratio. Similarly, we separate out the linear frequency dependence from the line-shape factors in the magnetic susceptibility by writing $\chi' = \omega\chi_0'$ and $\chi'' = \omega\chi_0''$. (see, for example, p. 31 of Ref. 23). The expressions for α_n are then given by

$$\bar{\alpha}_n = \frac{[f(\theta)]^2}{2\gamma^2 \rho v^3} \chi_0'' \frac{\omega^4}{1+\beta^2} \quad (17)$$

and

$$(\alpha_n)_{\text{MOUS}} = \frac{[f(\theta)]^2}{2\gamma^2 \rho v^3} (\chi_0'' - \beta\chi_0') \frac{\omega^4}{(1+\beta^2)^2} . \quad (18)$$

The angular dependence of the NAR absorption observed in aluminum[10] is in good agreement with that predicted by $[f(\theta)]^2$; this dependence was also

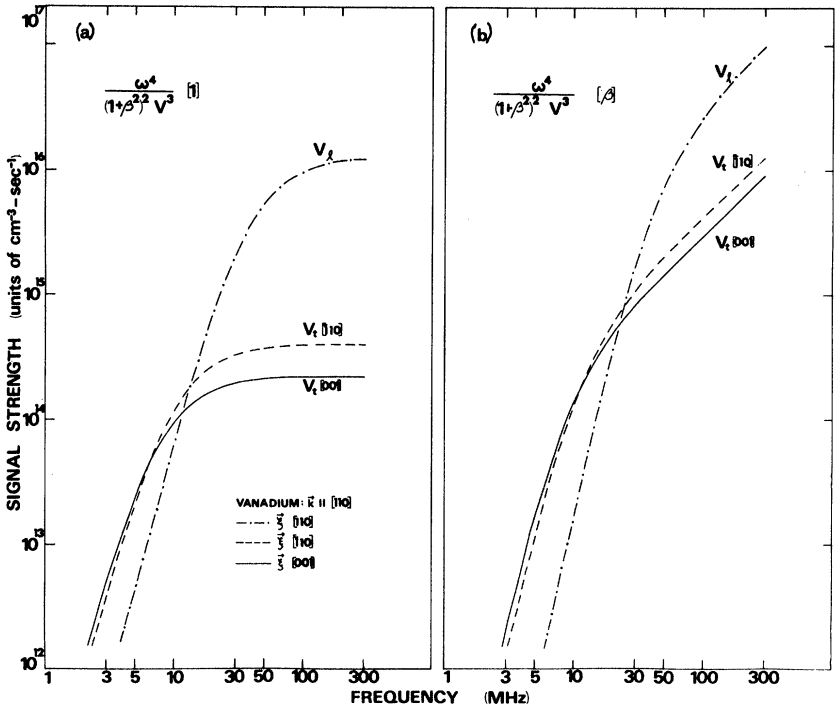

FIG. 8. Plot of theoretical values of $\omega^4[1]/(1+\beta^2)^2v^3$ (absorptive) and $\omega^4[\beta]/(1+\beta^2)^2v^3$ (dispersive) terms in $(\alpha_n)_{\mathrm{MOUS}}$ as a function of frequency for vanadium.

derived by Buttet *et al.* in Ref. 10. Equation (18) agrees with the corresponding expression [Eq. (3)] in Ref. 10 for the limiting case of $\beta = 0$ if we use the appropriate expression for χ_0''.[25] A comparison between Eqs. (17) and (18) indicates that for $\beta \ll 1$ the two methods of measuring α_n give the same results, i.e., α_n varies directly as $\omega^4\chi_0''$. For $\beta \gg 1$, however, $(\alpha_n)_{\mathrm{MOUS}}$ is proportional to $\chi_0'\omega$, while $\bar{\alpha}_n$ is proportional to $\chi_0''\omega^2$.

For frequencies sufficiently low or conductivities sufficiently high that the condition $\beta \ll 1$ is satisfied, the NAR signal from a MOUS is absorptive in character, i.e., proportional to χ_0'', and increases with frequency as ω^4. At intermediate frequencies or conductivities, such that β is comparable to unity, the NAR signal should be a mixture of absorption and dispersion and exhibits a more complicated dependence on frequency. For high frequencies or low conductivities the signal is dispersive in character and has a linear frequency dependence. For $\beta \ll 1$, $(\alpha_n)_{\mathrm{MOUS}}$ varies with velocity as v^{-3}. For $\beta \gg 1$, on the other hand, $(\alpha_n)_{\mathrm{MOUS}}$ varies as v^3. Since in many metals $v_l \simeq 2v_t$, this dependence of $(\alpha_n)_{\mathrm{MOUS}}$ on acoustic phase velocity favors the use of transverse waves in the low-frequency limit, and of longitudinal waves in the high-frequency limit. To illustrate the relative dependence of the absorptive and dispersive terms in $(\alpha_n)_{\mathrm{MOUS}}$ on frequency and velocity, the quantities $\omega^4[1]/(1+\beta^2)^2v^3$ and $\omega^4[\beta]/(1+\beta^2)^2v^3$ for vanadium have been calculated and plotted in Fig. 8. The cases illustrated are those for $\vec{k} \| [110]$, $\vec{\xi}[110]$, $\vec{\xi}[\bar{1}10]$, and $\vec{\xi}[001]$. The values of v and the constants used in calculating β are those given in Table II for 293 K. The preliminary reports of dipolar coupled NAR in aluminum[10] and vanadium[12] indicate that the data for $\beta \ll 1$ and $\beta \sim 1$ exhibit the features predicted above. No data have been reported in the $\beta \gg 1$ regime.

Our theoretical results for NAR dipolar coupling and experimental data on the Alpher-Rubin effect bear on the choice of techniques and materials for future NAR studies in metals. Assuming the availability of a suitable magnet, optimum signal-to-noise ratio would be achieved by the use of a high ultrasonic frequency, thus taking advantage of the favorable frequency dependence. For frequencies such that $\beta \geq 1$, however, signal strength increase with frequency may be more than offset by loss of sensitivity due to increased background ultrasound attenuation in the specimen.

ACKNOWLEDGMENT

We wish to thank Icheng Wu for aid in data analysis.

*Work supported in part by the National Science Foundation.

†Present address: Sandia Laboratories, Albuquerque, N. M. 87115.

[1] R. A. Alpher and R. J. Rubin, J. Acoust. Soc. Am. 26, 452 (1954).

[2]A. A. Galkin and A. P. Koroliuk, Zh. Eksperim. i Teor. Fiz. 34, 1025 (1958) [Soviet Phys. JETP 7, 708 (1958)].
[3]G. A. Alers and P. A. Fleury, Phys. Rev. 129, 2425 (1963).
[4]G. A. Alers, in *Physical Acoustics*, edited by W. P. Mason (Academic, New York, 1966), Vol. IV A.
[5]Y. Shapira and L. J. Neuringer, Phys. Rev. Letters 15, 724 (1965).
[6]D. J. Meredith, R. H. Watts-Tobin, and E. R. Dobbs, J. Acoust. Soc. Am. 45, 1393 (1969).
[7]Y. Shapira, in *Physical Acoustics*, edited by W. P. Mason (Academic, New York, 1968), Vol. V, gives an excellent review of this subject.
[8]E. H. Gregory and H. E. Bömmel, Phys. Rev. Letters 15, 404 (1965).
[9]R. E. Smith and D. I. Bolef, Phys. Rev. Letters 22, 183 (1969).
[10]J. Buttet, E. H. Gregory, and P. K. Baily, Phys. Rev. Letters 23, 1030 (1969).
[11]J. Buttet and P. K. Baily, Phys. Rev. Letters 24, 1220 (1970).
[12]P. K. Baily and H. E. Bömmel, Bull. Am. Phys. Soc. 15, 603 (1970).
[13]W. D. Smith, J. G. Miller, D. I. Bolef, and R. K. Sundfors, J. Appl. Phys. 40, 4967 (1969).
[14]S. Rodriguez, Phys. Letters 2, 271 (1962).
[15]M. J. Harrison, Phys. Rev. Letters 9, 299 (1962).
[16]S. Rodriguez, Phys. Rev. 130, 1778 (1963).
[17]J. J. Quinn and S. C. Ying, Phys. Letters 23, 61 (1966).
[18]J. J. Quinn, J. Phys. Chem. Solids 31, 1701 (1970).
[19]J. J. Quinn (private communication).
[20]M. H. Cohen, M. J. Harrison, and W. H. Harrison, Phys. Rev. 117, 937 (1960).
[21]W. D. Smith, Ph.D. dissertation, Washington University, St. Louis, Mo., 1970 (unpublished).
[22]E. H. Gregory, Bull. Am. Phys. Soc. 14, 401 (1969).
[23]W. D. Smith, J. G. Miller, R. K. Sundfors, and D. E. Bolef, J. Appl. Phys. (to be published).
[24]J. Buttet and E. H. Gregory (private communication).
[25]C. P. Slichter, *Principles of Magnetic Resonance* (Harper and Row, New York, 1963), p. 31.
[26]See, for example, R. Truell, C. Elbaum, and B. B. Chick, *Ultrasonic Methods in Solid State Physics* (Academic, New York, 1969).
[27]R. G. Leisure and D. I. Bolef, Rev. Sci. Instr. 39, 199 (1968).
[28]R. L. Melcher, D. I. Bolef, and J. B. Merry, Rev. Sci. Instr. 39, 1613 (1968).
[29]D. I. Bolef, in *Physical Acoustics*, edited by W. P. Mason (Academic, New York, 1966), Vol. IV A.

PHYSICAL REVIEW B VOLUME 3, NUMBER 5 1 MARCH 1971

Nuclear Resonance Study of Solid n-D_2†

J. H. Constable and J. R. Gaines
Department of Physics, The Ohio State University, Columbus, Ohio 43210
(Received 19 October 1970)

Pulsed nuclear-magnetic-resonance (NMR) experiments on solid n-D_2 samples have been performed over the temperature range 5–0.15 K. The spin-lattice relaxation time and second moments were measured as a function of temperature. No departures from Curie-law behavior were observed down to 0.15 K. Solid-echo techniques were used at several temperatures to demonstrate the contribution to the free-induction decay due to the $J=1$ molecules.

INTRODUCTION

A previous nuclear-magnetic-resonance (NMR) study[1] of the dependence of the longitudinal relaxation time T_1 upon the concentration of $J=1$ molecules in solid D_2 has shown that the magnetic properties of D_2 are analogous to those of HD doped with o-H_2 molecules.[2] In both systems, the sample consists of a mixture of molecules in the rotational states $J=0$ (o-D_2 or HD) and $J=1$ (p-D_2 or o-H_2). The nuclear spins of the $J=1$ molecules relax in a relatively short time to the energy reservoir provided by the rotational degrees of freedom,[3] which in turn is strongly coupled to the phonon modes in the solid. Since the spacings between the nuclear Zeeman energy levels in a large magnetic field are approximately equal for both $J=1$ and $J=0$ molecules, cross relaxation between the two-spin systems provides the mechanism by which the spin temperature of the $J=0$ molecules can relax to the lattice temperature. The direct coupling of the nuclear spins on the $J=0$ molecules to the lattice is very weak and can be neglected.[4] It is entirely possible, depending upon the relative concentration, that most of the observed NMR signal is due to $J=0$ molecules that have no direct relaxation mechanism to the lattice, and that the resonance of of the $J=1$ molecules is essentially unobservable except for its effect on the over-all relaxation behavior.

For n-D_2, two-thirds of the molecules have an even value of the rotational quantum number J ($J=0$ at low temperature) which must be associated with an even value of the total nuclear spin I ($I=2$ or $I=0$) according to the restrictions imposed on the total wave function by the Pauli principle. For the other third of the molecules, para-D_2, J is odd ($J=1$ at low temperatures) and the nuclear spin is